Journal of Southeast University (English Edition) Vol. 41, No. 4, pp. 465-472 Dec. 2025 ISSN 1003-7985

Combined recovery technology of pile foundations for offshore wind turbines

DING Hongyan, TIAN Xiaoxuan, ZHANG Puyang, XIN Lianshuo, LE Conghuan

(State Key Laboratory of Hydraulic Engineering Intelligent Construction and Operation, Tianjin University, Tianjin 300072, China)

Abstract: In recent years, offshore wind turbines have rapidly developed, and many pile foundations installed earlier are now approaching decommissioning. Thus, the efficient removal of pile foundations has become a critical issue for the sustainable development of offshore wind energy. To address this issue, this paper systematically investigates three methods for the recovery of pile foundations using physical model experiments: water injection + lifting, air injection + lifting, and air retention + water injection. The experimental results show that the water injection + lifting method exhibits remarkable advantages in recovering large-diameter and inclined pile foundations; however, realigning inclined piles during recovery remains challenging, and a risk of pile overturning exists. The air injection + lifting method proves effective for realigning inclined piles but presents a risk of air expulsion failure, which may affect the continuity and stability of the recovery process. By contrast, the air retention + water injection method combines the characteristics of water injection and air injection techniques, effectively avoiding air expulsion failure and exhibiting pronounced displacement jumps during pile uplift. These findings provide a valuable reference for future decommissioning practices of offshore wind pile foundations, offer important engineering application value, and contribute positively to the sustainable development of the offshore wind industry.

Key words: offshore wind turbine; pile foundation; recovery; physical model experiment

DOI: 10. 3969/j. issn. 1003-7985. 2025. 04. 008

Against the background of the "carbon emission peak" and "carbon neutrality" goals, many countries have begun to develop energy systems primarily based on clean energy. In 2020, China formally proposed the targets of "carbon peak" and "carbon neutrality," signaling that green development within the energy sector has become a new trend[1-2]. With continuous enhancement in environmental awareness, the wind power industry, a crucial component of the clean energy sector, has experienced rapid growth in recent years[3]. Among its various forms, offshore wind power generation—characterized by high efficiency, environmental cleanliness, and considerable development potential—has become one of the key directions for global new energy development[4].

As offshore wind power rapidly develops, the decommissioning of wind turbines has become an increasingly important concern. Monopile foundations, which are the most widely used foundation type in offshore wind farms worldwide, offer several key advantages, including minimal seabed occupation, high load-bearing capacity, structural stability, and low, uniform settlement[5]. Currently, the technology for pile foundations remains underdeveloped. At present, most wind farms typically use the cutting pile method to remove the portion of the foundation above the seabed. This approach has highlighted the urgent need for more efficient and comprehensive removal techniques

Ge et al. [6] used model testing methods to compare the load-bearing characteristics of conventional pull-out piles and root-type pull-out piles in sandy soils under vertical uplift loads. Sun et al. [7] performed indoor pull-out tests on 12 steel pipe piles, divided into 4 groups, under different uplift loads based on a specific similarity ratio. In 2018, "The BLUE Piling" experimental tests conducted in the Netherlands partially validated the feasibility of negative pressure uplift recovery. Beuckelaers et al. [8] proposed a finite element limit analysis method for the rapid evaluation of the excess pressure required for hydraulic extraction of pile foundations. The method accounts for mechanisms such as inner and outer pile-soil interface friction and plug failure, and is applicable to layered soil conditions.

This study employs physical model experiments to investigate three combined removal processes for vertical monopile foundations: water injection + lifting, air injection + lifting, and a combination of air retention and water injection. The study clarifies the interaction mechanisms between the monopile and the surrounding soil during the removal process. Furthermore, the study determines the required pressures for foundation removal and fits pressure-displacement curves to characterize the removal process.

Received 2025-03-01, **Revised** 2025-04-21.

Biographies: Ding Hongyan (1963—), male, doctor, professor; Zhang Puyang (corresponding author), male, doctor, professor, zpy_td@163. com.

Foundation item: The National Natural Science Foundation of China (No. 52171274).

Citation: DING Hongyan, TIAN Xiaoxuan, ZHANG Puyang, et al. Combined recovery technology of pile foundations for offshore wind turbines[J]. Journal of Southeast University (English Edition), 2025, 41(4): 465-472. DOI: 10. 3969/j. issn. 1003-7985. 2025. 04. 008.

1 Physical Model Experiment

1.1 Prototype and experimental conditions

To aid readers in understanding the terminology used in the subsequent sections, the relevant terms and their specific definitions are presented in Table 1.

This study primarily focuses on large-diameter monopile foundations, as well as shallow-depth monopiles deployed in early-stage offshore wind farms. The relevant parameters for several representative prototype foundations are presented in Table 2.

Table 1 Glossary of terms related to experiments and analysis

Term	Definition
Water injection	Injecting water into the pile through the pile top cover
Air injection	Injecting air into the pile through the pile top cover
Air retention	Trapped air in the upper part of the pile after embedment
Lifting	The counterweight connects to the lifting ring on the pile top cover to apply tensile force.
Cabin pressure	Internal pressure inside the pile after embedment
Pile foundation displacement	The vertical distance the pile moves upward

Table 2 Prototype foundation parameters

Prototype foundation	Foundation diameter/m	Embedment depth/m
The 500 kW two-bladed wind turbines at the Lely wind farm in the Netherlands	3.7	15
A wind farm in Jieyang, Guangdong, China	8.7	35-40
A wind farm in Zhuanghe, Fujian, China	8.2	31
The H5 wind farm operated by Guoneng Group in Yancheng, Jiangsu, China	8.2	40

Based on the above analysis, the experimental conditions were designed with pile diameter and embedment depth as the primary variables. The specific parameters are presented in Table 3.

Table 3 Experimental conditions

Condition	Foundation diameter/cm	Embedment depth/cm	External load/kg	Air retention/cm
W-D20H80	20	80	0	0
W-D20H80-10kg	20	80	10	0
W-D20H70-10kg	20	70	10	0
W-D20H65-10kg	20	65	10	0
W-D25H80-5kg	25	80	5	0
W-D20H80-5kg	20	80	5	0
A-D20H80	20	80	0	0
A-D20H80-5kg	20	80	5	0
A-D25H80-5kg	25	80	5	0
D20H80	20	80	0	0
D20H80-A10cm	20	80	0	10
D20H80-A20cm	20	80	0	20
D20H80-A30cm	20	80	0	30
D20H80-A40cm	20	80	0	40

Note: The letter W denotes water injection, and A denotes air injection. The letter D represents the pile diameter, while H refers to the pile embedment depth. 5kg (10kg) indicates a fixed counterweight. A10cm (A20cm/A30cm/A40cm) indicates that 10 cm (20 cm/30 cm/40 cm) of air is retained within the pile.

1.2 Experimental procedure

The sand used in the experiment was Fujian standard sand and the grain size ranges from 0.1 to 2.0 mm, with a relative density of 0.58, an elastic modulus of 18 MPa, an internal friction angle of 32.5°, a maximum dry density of 1.5 g/cm^3, a minimum dry density of 1.1 g/cm^3, and a permeability coefficient of 0.068 cm/s.

The model tests were conducted with a geometric similarity ratio of 1∶40. The height of the pile foundation model was 1.2 m, with a wall thickness of 5 mm and diameters of 0.15, 0.20, and 0.25 m, corresponding to masses of 6.70, 9.15, and 11.90 kg. To facilitate the pressurized removal experiments, a steel top cover was installed at the top of the model. The cover was designed with a flange and two water pipe interfaces with a diameter of 8 mm, as well as openings for the installation of pore pressure transducers.

1.2.1 Water injection + lifting recovery

The experimental setup is shown in Fig. 1. The monopile foundation is preinstalled in saturated experimental sand, with the top plate of the foundation connected to pore pressure sensors and an inclinometer. A water pipe is connected to the injection port, while steel cables are routed over two fixed pulleys. One end of each steel cable is attached to the lifting ring on the top plate of the foundation, and the other end is fixed with two 2.5 kg counterweights. The water injection + lifting recovery process is shown in Fig. 2.

Fig. 1 Schematic of recovery equipment setup

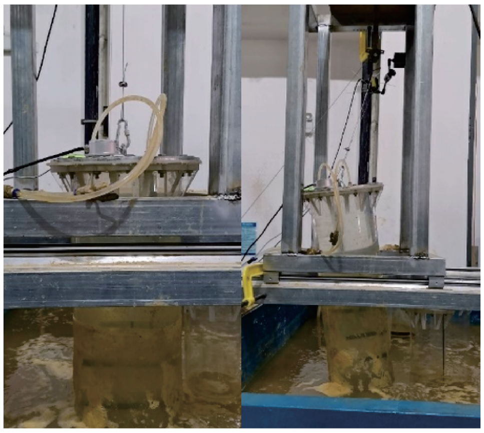

Fig. 2 Water injection + lifting recovery process

1.2.2 Air injection + lifting recovery

The air injection + lifting recovery process is illustrated in Fig. 3. Under the combined action of internal air pressure and the upward lifting force generated by the counterweights, the monopile foundation exhibits vertical displacement. Notably, at the conclusion of the air injection + lifting recovery experiment, the monopile foundation typically remains upright, showing little to no inclination.

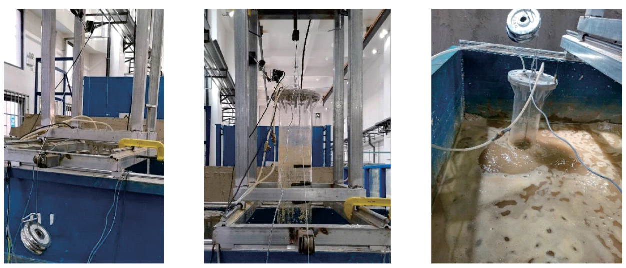

(a) (b) (c)

Fig. 3 Air injection + lifting recovery process. (a) During recovery; (b) Recovery endpoint; (c) Recovery failure

1.2.3 Air retention and water injection recovery

In this set of experiments, the water injection pipe, pressure sensor, and inclinometer are connected to the top cover of the pile. The experimental phenomenon reveals a distinct jumping pattern in the displacement behavior of the pile foundation. Continuous water injection into the pile ensures that the water remains in the pile chamber, thereby preventing the air release damage. Furthermore, as a certain amount of air is stored inside the chamber, the pile foundation can maintain its stability and it does not become difficult to straighten during tilting.

2 Experimental Results

2.1 Water injection + lifting recovery

2.1.1 Recovery curves of pile foundations with different lifting forces

The recovery curves for the water injection + lifting method are compared in Fig. 4. It is observed that the chamber pressure for the W-D20H80-5kg and W-D20H80-10kg conditions is generally lower than that for the W-D20H80 condition. Based on the experimental data, the following preliminary conclusions can be drawn: (1) the application of lifting force effectively reduces the chamber pressure required for water injection recovery of the pile foundation, and (2) the application of lifting force does not affect the slope of the pressure reduction curve.

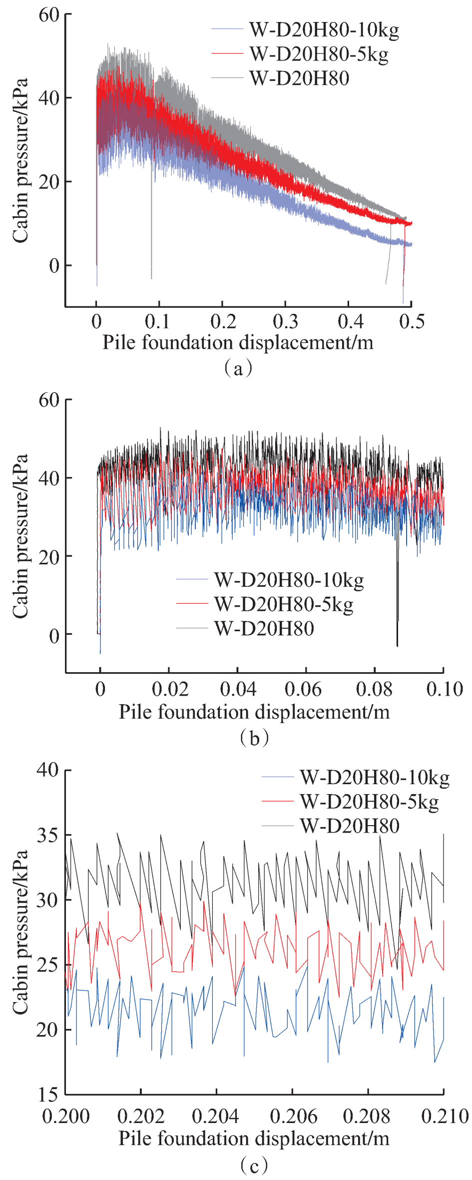

Fig. 4 Comparison of water injection + lifting recovery curves for W-D20H80. (a) Overall curve; (b) Initiation curve; (c) Detailed curve

2.1.2 Recovery curves of pile foundations with different mud insertion depths

The recovery curves for pile foundations with different mud insertion depths using the water injection + lifting method are shown in Fig. 5. From the overall curve, similar to water injection recovery, the required chamber pressure decreases as the mud insertion depth decreases. Furthermore, upon examining the detailed curves, the pressure reduction profiles for the W-D20H80-5kg and W-D20H65-5kg conditions are observed to be nearly parallel.

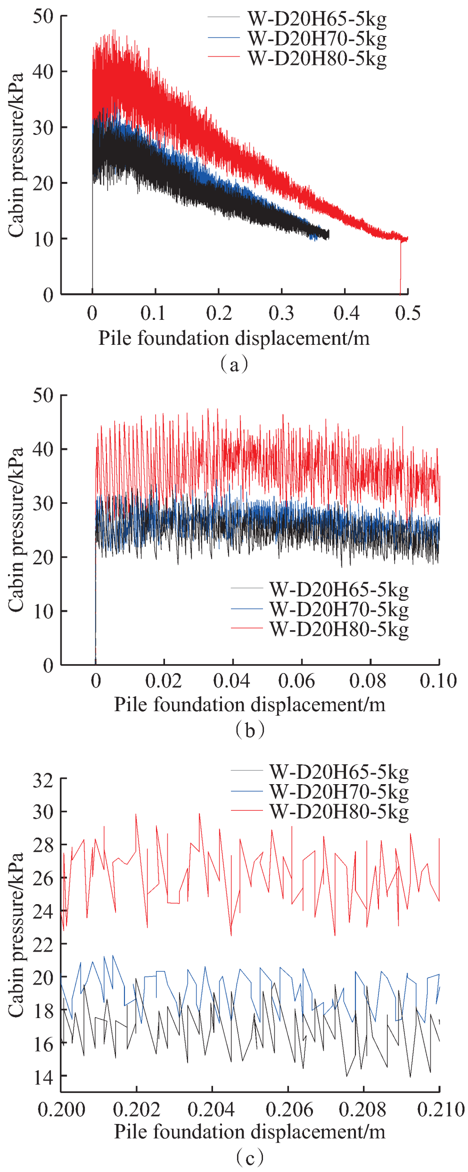

Fig. 5 Comparison of water injection + lifting recovery curves for different mud insertion depths. (a) Overall curve; (b) Initiation curve; (c) Detailed curve

2.1.3 Recovery curves of pile foundations with different diameters

The recovery curves for pile foundations with different diameters using the water injection + lifting method are shown in Fig. 6. From the overall curve, the chamber pressure during recovery for the W-D25H80-5kg condition remains consistently lower than that for the W-D20H80-5kg condition. A closer examination of the detailed curve reveals that the W-D25H80-5kg condition exhibits a higher fluctuation frequency, albeit with a smaller fluctuation amplitude than the W-D20H80-5kg condition.

2.2 Air injection + lifting recovery

2.2.1 Recovery curves of pile foundations with different lifting forces

As shown in Fig. 7, the recovery curve for the A-D20H80-5kg condition shows an overall lower chamber pressure than the A-D20H80 condition. Based on the above experimental results, the following preliminary conclusions can be drawn: (1) the application of lifting force effectively reduces the chamber pressure required for recovery, and (2) the slope of the pressure reduction curve is not affected by the lifting force.

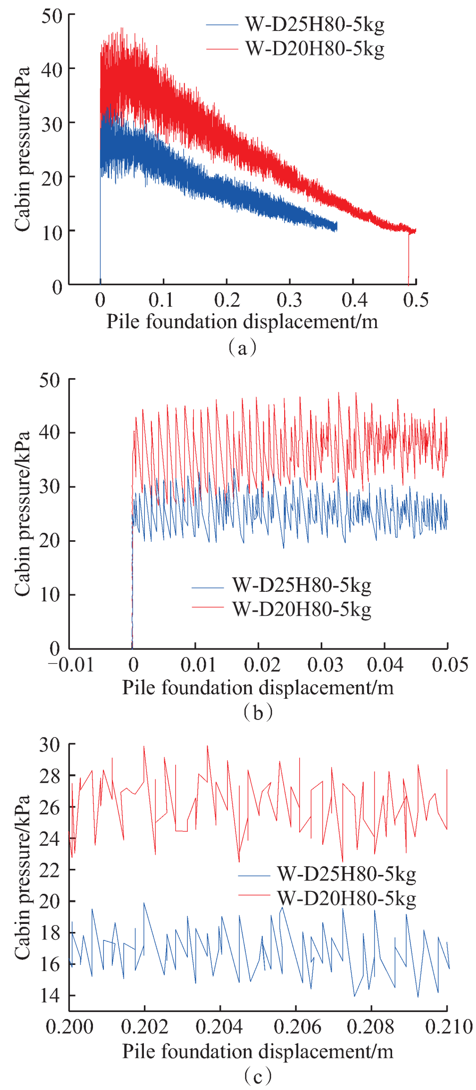

Fig. 6 Comparison of water injection + lifting recovery curves for pile foundations with different diameters. (a) Overall curve; (b) Initiation curve; (c) Detailed curve

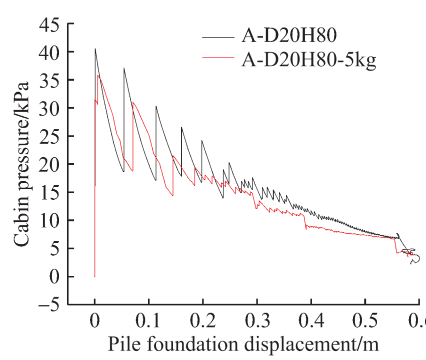

Fig. 7 Comparison of air injection + lifting recovery curves for W-D20H80

2.2.2 Recovery curves of pile foundations with different diameters

The recovery curves for pile foundations with different diameters are compared in Fig. 8. The initial chamber pressure for the A-D20H80-5kg condition is approximately 35 kPa, whereas that for the A-D25H80-5kg condition is approximately 25 kPa. In terms of curve fluctuation patterns, the A-D20H80-5kg condition exhibits a lower fluctuation frequency and a greater fluctuation amplitude than the A-D25H80-5kg condition.

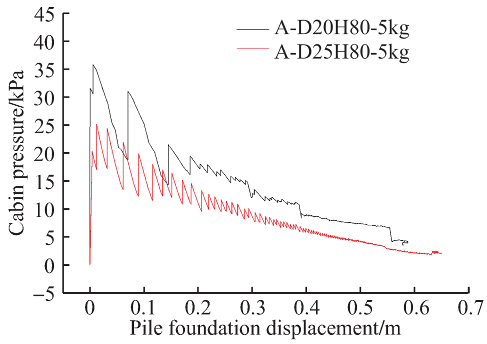

Fig. 8 Air injection + lifting recovery curves for pile foundations with different diameters

2.3 Air retention and water injection recovery

The recovery curves for different initial air retention heights using the air retention and water injection method are shown in Fig. 9. It can be observed that recovery required a lower chamber pressure under conditions with retained air than under those without. This indicates a gradual transition from water injection recovery to air injection recovery.

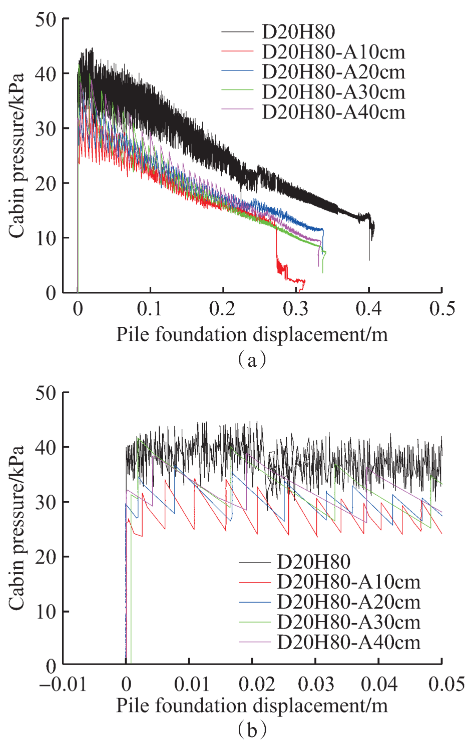

Fig. 9 Recovery curves for different initial air retention heights under the air retention and water injection method. (a) Overall curve; (b) Initiation curve

3 Theoretical Derivation

3.1 Water injection + lifting recovery

This section's theoretical derivation is based on water injection recovery theory[9]. The key formula is the calculation of the breakthrough pressure P_b for a foundation with a mud insertion depth h, as given by the following equation:

$$P_b = \frac{Q_f + G}{A} = \frac{\pi D\beta\left(a_i \frac{Q}{kA}\gamma_w + \gamma'\right)H^2}{2A} + \frac{G}{A} \quad (1)$$

where Q_f is the lateral frictional resistance acting on the pile foundation; G is the weight of the pile foundation; A is the area of the top surface of the pile foundation; D is the diameter of the pile; β is the dimensionless friction parameter, considered as 0.29; a_i is the proportion of internal wall frictional resistance; Q is the water pump flow rate or seepage flow rate; k is the permeability coefficient of the soil within the pile shaft; γ_w is the unit weight of water; γ' is the buoyant unit weight of the soil; H is the mud insertion depth of the pile.

The formula for calculating the displacement distance x_h of the pile foundation at the next stage when the mud insertion depth is h is as follows:

$$x_h = \frac{2b}{a},\quad a = \frac{KA}{m},\quad b = \frac{(1-\gamma)Q_{fh}}{m} \quad (2)$$

where K is the slope of the pressure reduction curve; m is the mass of the pile foundation; γ is the coefficient of sliding friction; Q_{fh} is the lateral frictional resistance.

Based on the experimental data, Eq. (1) is modified, yielding the following results:

$$P_b = \frac{Q_f + G - F}{A} = \frac{\pi D\beta\left(a_i \frac{Q}{kA}\gamma_w + \gamma'\right)H^2}{2A} + \frac{G - F}{A} \quad (3)$$

where F is the tensile force applied to the top cap of the monopile foundation.

Eqs. (2) and (3) are used to fit the water injection + lifting recovery curve. The parameters selected for the fitting process are shown in Table 4, and the fitting results are presented in Fig. 10.

Table 4 Fitting parameter values for water injection + lifting recovery

Parameter	W-D20H80	W-D25H80	W-D20H70	W-D20H65
Sliding friction coefficient γ	0.7	0.7	0.7	0.7
Pressure reduction slope $K/10^6$	13	13	13	13
Chamber pressure amplification factor E	1.2	1.0	1.2	1.2

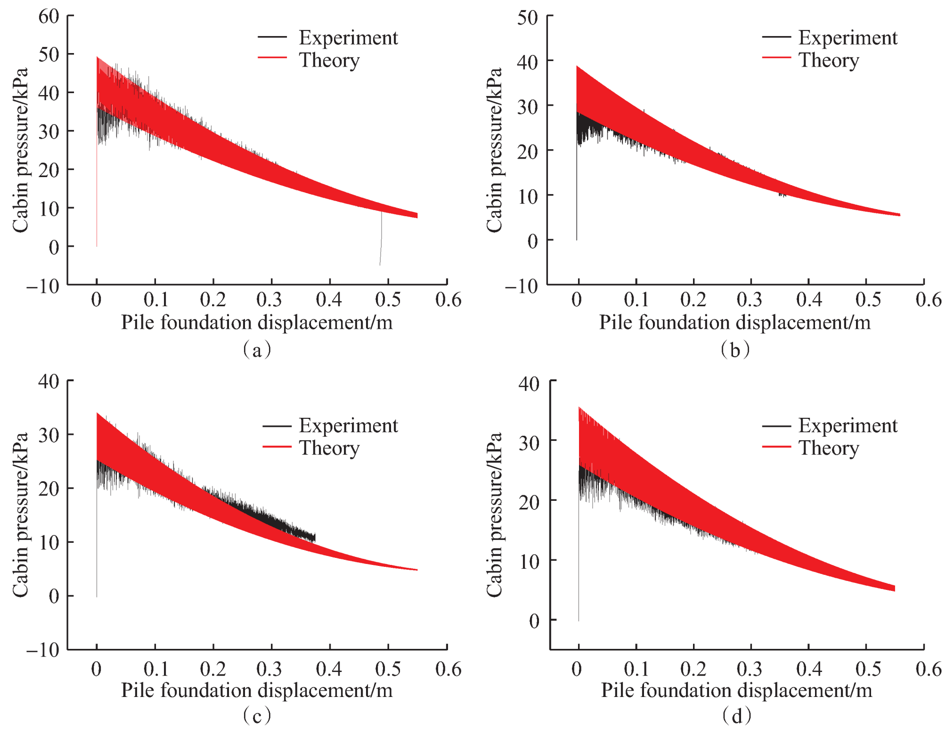

Fig. 10 Fitting results of water injection + lifting recovery curves. (a) W-D20H80-5kg; (b) W-D20H70-5kg; (c) W-D20H60-5kg; (d) W-D25H80-5kg

3.2 Air injection + lifting recovery

This section's theoretical derivation is based on the air injection recovery theory[10]. The key formula is the calculation of the breakthrough pressure P_A for a foundation with a mud insertion depth h, as given by the following equation:

$$P_A = \frac{\pi D\beta\gamma' H^2 + 2G}{2A - \pi D\beta a_i a_s NH} \tag{4}$$

where a_s is the seepage conversion coefficient, and N is the water-to-air conversion coefficient.

The formula for calculating the displacement distance x_h of the pile foundation at the next stage when the mud insertion depth is h is as follows:

$$x_h = \frac{2b}{a},\quad a = \frac{KA}{m},\quad b = \frac{(1-\gamma)Q_{fh}}{m} \tag{5}$$

Based on the experimental data, the formula (4) is modified, yielding the following results:

$$P_A = \frac{\pi D\beta\gamma' H^2 + 2G}{2A - \pi D\beta a_i a_s bH} - \frac{F}{A} \tag{6}$$

Using Eqs. (5) and (6), the air injection + lifting recovery curve is fitted. The fitting results are presented in Table 5, and the parameters selected for the fitting process are illustrated in Fig. 11.

Based on the experimental data and curve fitting results, it is found that the air injection recovery theory still demonstrates strong applicability in the air injection + lifting recovery process.

Table 5 Air injection recovery parameter values

Parameter	A-D20H80-5kg	A-D25H80-5kg
Internal friction proportion a_i	0.49	0.49
Seepage conversion coefficient a_s	0.76	0.76
Water-to-air conversion coefficient N	0.8	0.8
Pressure reduction slope K	400	350
Chamber pressure amplification factor E	1.2	1.3
Displacement reduction coefficient C	0.9	0.6

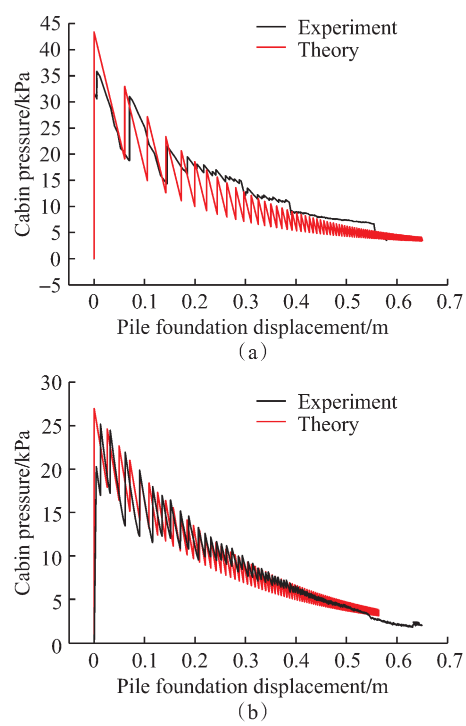

Fig. 11 Comparison of air injection + lifting recovery curve fitting results. (a) A-D20H80-5kg; (b) A-D25H80-5kg

3. 3 Air retention + water injection recovery

This section's theoretical derivation is based on the recovery theory presented in Section 3. 2. The focus is on studying the influence of varying air retention heights on the slope of the pressure reduction curve and the displacement fluctuation characteristics of the pile foundation. Utilizing the recovery theory articulated in Section 3. 2, the recovery curve for air retention and water injection is fitted. The fitting results are shown in Fig. 12, with the parameters selected for the fitting process listed in Table 6.

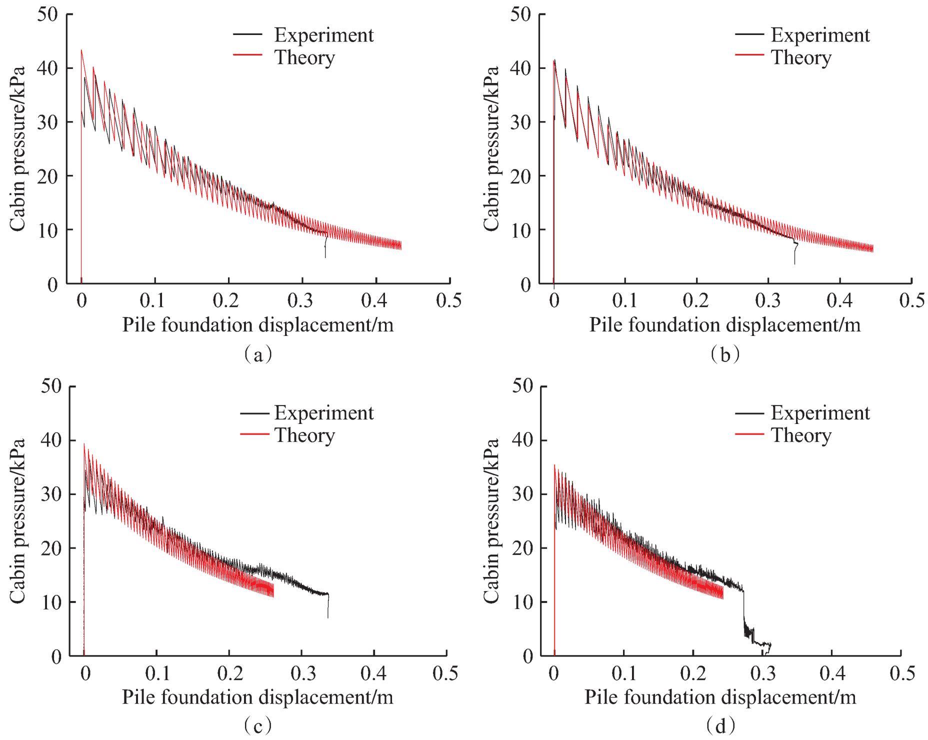

Fig. 12 Fitting results of air retention and water injection recovery curve. (a) D20H70-A40cm; (b) D20H70-A30cm; (c) D20H70-A20cm; (d) D20H70-A10cm

Table 6 Parameter values for air retention and water injection recovery

Parameter	Air retention/cm			
	40	30	20	10
Internal friction proportion a_i	0.49	0.49	0.49	0.49
Seepage conversion coefficient a_s	0.76	0.76	0.76	0.76
Water-to-air conversion coefficient N	0.8	0.8	0.8	0.8
Pressure reduction slope K	800	700	1 300	1 700
Chamber pressure amplification factor E	1.10	1.05	1.10	1.00
Displacement reduction coefficient C	0.4	0.4	0.8	0.7

4 Conclusions

Through physical model experiments, this study investigates the water injection + lifting recovery process, the air injection + lifting recovery process, and the air retention + water injection recovery process. The objective is to understand the interrelationships of these recovery processes and explore more optimal combined processes. The water injection + lifting recovery process inherits the advantages of water injection recovery in the context of large-diameter pile foundation recovery and inclined pile foundation recovery. Similarly, the air injection + lifting recovery process inherits the advantages of air injection recovery in large-diameter pile foundation and inclined pile foundation recovery.

References

[1] CAI S, HAN D Q, CHA J R. Empirical research on vertical greening and energy saving technology in the range of architectural boundaries[J]. Journal of Southeast University (English Edition), 2023, 39(1): 33-48.

[2] ZHANG P Y, ZHANG L Y, XIONG L C, et al. Influence of inflow conditions on the hydrodynamic characteristics of floating photovoltaic membrane structures[J]. Journal of Southeast University (English Edition), 2024, 40(4): 363-371.

[3] ZHANG P Y, XIONG L C, LE C H, et al. Comparison

analysis of the bearing capacity of rock-socketed piles and sand piles for offshore wind turbines [J]. Journal of Southeast University (English Edition), 2023, 39 (4): 384-392.

[4] LI Z Y, DAI G L, DU S, et al. Experimental study on scour resistance characteristics of fluid cured soil for offshore wind power foundation [J]. Journal of Southeast University (Natural Science Edition), 2023, 53 (4): 647-654. (in Chinese)

[5] NIELSEN B H. Feasibility study of the complete removal of monopiles using vibratory pile removal [D]. Trondheim, Norway: Norwegian University of Science and Technology, 2022.

[6] GE N, SUN Y, HOU C Q, et al. Model test on rooted uplift pile in sand [J]. Journal of Yangtze River Scientific Research Institute, 2019, 36(8): 146-152. (in Chinese)

[7] SUN T T, YANG J X, ZHANG Z H, et al. Experimental study on uplift piles with different diameters and lengths in clay [J]. Journal of Highway and Transportation Research and Development, 2021, 38(10): 44-53. (in Chinese)

[8] BEUCKELAERS W J, VANDENBOER K, VERBRAECKEN J, et al. One-dimensional finite element limit analysis for hydraulic pile extraction [J]. Computers and Geotechnics, 2021, 133: 104042.

[9] ZHANG P Y, XIN L S, DING H Y, et al. Research on water injection demolition method for offshore pile foundation [J]. Journal of Tianjin University (Science and Technology), 2024, 57(4): 437-444. (in Chinese)

[10] XIN L S. Study on removal technology of offshore wind power pile foundation [D]. Tianjin: Tianjin University, 2023. (in Chinese)

海上风电桩基础的联合回收技术

丁红岩，田晓轩，张浦阳，信连硕，乐丛欢

（天津大学水利工程智能建设与运维全国重点实验室，天津300072）

摘要：近年来海上风电快速发展，而安装时间较久的单桩基础即将迎来退役，因此如何高效拆除单桩基础成为海上风电持续发展的关键问题。针对这一需求，本文通过物理模型试验，系统研究了注水+吊装、注气+吊装和留气注水3种回收桩基础的方法。试验结果表明：注水+吊装工艺在回收大直径桩基础和倾斜桩基础方面具有明显优势，但对于倾斜桩，回收过程中扶正难度较高，桩基础存在倾覆的风险；注气+吊装工艺能有效扶正倾斜桩基础，但在回收过程中存在排气破坏的风险，影响回收的连续性和稳定性；留气注水工艺兼具注水与注气工艺的特点，有效避免了排气破坏，在桩基础顶升方面具有较强的位移跳跃性。研究成果为未来海上风电桩基础的退役提供了参考，具有一定的工程应用价值，对于推动海上风电行业的可持续发展具有积极意义。

关键词：海上风电；桩基础；回收；物理模型试验

中图分类号：TU449